International Journal of General Medicine

Dovepress
Taylor & Francis Group

Open Access Full Text Article

ORIGINAL RESEARCH

Glycosylation-Related Genes and Prognostic Signatures in Diabetic Nephropathy

Xiaohui Li[1], Tao Sun[2], Xiaoqian Li[1], Huangmin Li[1], Xuejun Zheng[1], Yiding Zhang[1], Wei Yu[1], Yifei Liu[3], Jin Shang[1], Jing Xiao[1], Zhanzheng Zhao[1]

[1]Department of Nephrology, The First Affiliated Hospital of Zhengzhou University, Zhengzhou, Henan, 450052, People's Republic of China; [2]Henan Medical College, Zhengzhou, Henan, 451191, People's Republic of China; [3]Department of Nephrology, The Second Xiangya Hospital, Central South University, Changsha, Hunan, 410011, People's Republic of China

Correspondence: Jing Xiao; Zhanzheng Zhao, Email xiaojing5123@139.com; zhanzhengzhao@zzu.edu.cn

Background: Diabetic nephropathy (DN) is the leading cause of end-stage renal disease worldwide, whose pathogenesis involves immune dysregulation and inflammatory response. Glycosylation plays key roles in numerous biological processes. This study aims to interrogate the role of glycosylation-related genes in tubulointerstitial immunoinflammatory injury in DN.

Methods: We utilized two tubulointerstitial transcriptome datasets from DN patients and normal individuals. Glycosylation-related hub genes were identified by integrating differential expression analysis, glycosylation-related gene sets, and machine learning. Immune cell infiltration was assessed using single-sample GSEA (ssGSEA), and functional enrichment analysis was performed via GO and KEGG. The expression levels of hub genes were validated in STZ-induced diabetic mouse model (n=5/group) followed by the evaluation of diagnostic efficiency and clinical significance.

Results: Six glycosylation-related hub genes (HEXB, B4GALT5, GALNT7, GCNT3, CGA, and VCAN) were identified, all closely associated with immune cell infiltration in DN. Enrichment analysis indicated their involvement in immune and inflammatory processes. CGA was significantly downregulated, while the other genes were upregulated in DN, which was experimentally validated in diabetic mice. ROC curve analysis revealed high diagnostic accuracy for all genes: HEXB (AUC = 0.892), B4GALT5 (AUC = 0.909), GALNT7 (AUC = 0.931), GCNT3 (AUC = 0.929), CGA (AUC = 0.898), and VCAN (AUC = 0.967). Elevated VCAN, GCNT3, and GALNT7 exhibited a positive association with renal function decline or proteinuria, providing valuable prognostic insights.

Conclusion: This study highlights the significant role of glycosylation-related genes in DN pathogenesis, likely mediated through immune and inflammatory mechanisms. VCAN, GCNT3, and GALNT7 show particular promise as novel biomarkers for clinical diagnosis and immunotherapeutic targets, supporting their future clinical translation for DN management.

Keywords: diabetic nephropathy, glycosylation, bioinformatics analysis, immune infiltration

Introduction

Diabetic nephropathy (DN) is characterized by increased production of advanced glycation end products (AGEs), which trigger reactive oxygen species generation, subsequent inflammatory response and renal fibrosis.[1,2] It is known that over 70% of proteins are glycosylated, which adds a carbohydrate to a protein or lipid carrier, thereby exerting influence upon protein stability, folding, subcellular localization and function.[3,4] Glycosylation has been increasingly recognized as a key modulator in the pathogenesis of kidney diseases. Previous investigations have primarily focused on its role in podocyte dysfunction, tubular injury, and the accumulation of glycosylated extracellular matrix proteins, which contribute to fibrosis and a decline in glomerular filtration rate.[5,6] Building upon this established context, it is reported that circulating AGEs can predict kidney function decline and high-risk chronic kidney disease in individuals with chronic type 2 diabetes.[7] It has been reported that increased circulating levels of AGEs were strongly associated with the progression of DN. Mechanistically, AGEs can give rise to renal pathological phenotype in DN, including the thickening of the GBM, glomerulosclerosis and cell damage.[8] Emerging evidence has proven that IgG glycans are highly implicated in many metabolic diseases, including dyslipidemia, type 2 diabetes and diabetic nephropathy.[9–12] Glycosylation of proteins can

Received: 7 June 2025
Accepted: 27 October 2025
Published: 22 November 2025

be classified into two types: O-glycosylation and N-glycosylation. N-glycosylation is associated with a covalent bond formation between N-sugar chain and NH2 group of aspartic acid, while O-glycosylation is associated with a covalent bond formation between O-sugar chain and OH group of serine or threonine. However, glycosylation has not been fully elucidated in the field of DN. Plasma IgG N-glycosylation, particularly galactosylation and sialylation, is related to a higher prevalence of diabetic nephropathy. Differential IgG glycans are observed between healthy individuals and diabetic nephropathy patients.[10,11] In addition, the patterns of IgG glycosylation in type 2 diabetes reveal a faster kidney function decline.[12] C3 N-glycome is enhanced in T1D patients with severe albuminuria and was parallel to increased HbA1c levels.[13] A single-cell LacNAc sequencing reveals that glycosylation levels in neutrophils were significantly increased in the T2DM and T2DKD groups relative to HC subjects. Further scrutiny revealed that this alteration was especially enriched in LDG subpopulations, indicating glycosylation abrogates the normal execution of neutrophil death programs.[14] This study aims to move beyond conventional analyses by integrating transcriptomic data from DN patients to identify glycosylation-related hub genes and, innovatively, to explore their correlation with immune cell infiltration. This combined approach provides a fresh perspective on the disease's pathology and unlocks new avenues for immunomodulatory therapies.

Methods

Datasets Collection

The gene expression profiling data were downloaded in October 2024 from Gene Expression Omnibus (GEO, http://www.ncbi.nlm.nih.gov/geo). GSE30529, a microarray dataset based on GPL571 platform ([HG-U133A_2] Affymetrix Human Genome U133A 2.0 Array), includes renal tubulointerstitium from 10 DN patients and 12 normal individuals. GSE104954, a microarray dataset based on GPL22945 platform ([HG-U133_Plus_2] Affymetrix Human Genome U133 Plus 2.0 Array [CDF: Brainarray HGU133Plus2_Hs_ENTREZG_v19]), includes renal tubulointerstitium from 18 DN patients and 7 normal individuals. Glycosylation-related gene set, which contains 572 genes, was derived from the GSEA Website (http://www.gsea-msigdb.org).

Differential Gene Expression Analysis

Two datasets were subjected to quantile normalization using the R preprocessCore package. Differential expression analysis was performed by the limma package in R language. Volcano plot and heatmap were generated for differential expression analysis by ggplot2. Genes with $|logFC| > 0.5$ and $P < 0.05$ were selected as differentially expressed genes (DEGs). Among them, genes with $logFC > 0.5$ were considered upregulated, and those with $logFC < -0.5$ were considered downregulated.

Enrichment Analysis

The enriched Gene Ontology (GO) terms include molecular function (MF), biological process (BP) and cellular component (CC). Kyoto Encyclopedia of Genes and Genomes (KEGG) analysis was performed to elucidate the significant pathways involved. These enrichment analyses were carried out to analyze DEGs and glycosylation-related genes for functional and pathway enrichment analysis by clusterProfiler packages in R.

Identification of Glycosylation-Related Hub Genes in DN Patients

Two datasets were integrated, and removal of batch effect was performed using limma and sva R packages. Principal component analysis (PCA) plot was generated by FactoMineR and factoextra packages. To further narrow down the hub genes, machine learning algorithms, including LASSO regression and random forest, were employed.

Subsequently, we denoted the intersection of glycosylation-related genes and the two machine learning methods as final hub genes and used these hub genes for subsequent analysis. We then analyzed the correlation between hub genes by circlize package in R. ROC curves were created by pROC package to estimate the efficiency of hub genes for the diagnosis of DN.

Correlation Analysis Among Glycosylation-Related Hub Genes and Immune Landscape in DN

To evaluate the infiltration levels of immune cells in each sample, we used the ssGSEA function in the R package Gene Set Variation Analysis (GSVA). Marker genes of immune cell types for ssGSEA were obtained from Bindea et al[15] and provided as an additional file (Supplementary Table S1). We investigated the correlations among different types of DN-infiltrating immune cells. Then, the correlation between the identified hub genes and the abundance of these immune cells was assessed using the Pearson correlation analysis.

Construction of Co-Expression Network and Gene Set Enrichment Analysis (GSEA)

Co-expression of hub genes was performed, and the top50 positively correlated genes were displayed through the heat maps. Based on these significant co-expressed genes, Gene Set Enrichment Analysis (GSEA) was conducted using the Reactome database.

Predicted Upstream Transcriptional Regulators of Hub Genes

To query the potential upstream regulators of these hub genes, RegNetwork database (https://regnetworkweb.org/) was used to explore upstream transcription factors and miRNAs, and the results were visualized through cytoscape software. Hub genes in the regulatory network were demarked by yellow circles.

Immunohistochemistry

The kidney tissues from Streptozotocin (STZ)-induced diabetic nephropathy mice were embedded in paraffin, and then sliced into 4-μm-thick sections for immunohistochemical staining. After dewaxing and rehydration, microwave antigen retrieval and endogenous peroxidase blocking were followed. Next, the sections were subjected to incubation with antibodies against HEXB (DF3074, Affinity, 1:100), CGA (DF6371, Affinity, 1:100), VCAN (ab270445, Abcam, 1:200), B4GALT5 (DF3841, Affinity, 1:200), GCNT3 (DF14166, Affinity, 1:100), GALNT7 (GB114693-100, Servicebio, 1:400), and HRP-conjugated secondary antibodies. The color reaction was developed with 3,3-diaminobenzidine (DAB). Nuclear counterstaining was carried out with Mayer's hematoxylin. Quantitative image analysis of IHC was conducted using the image analysis software Image-Pro plus version 6.0. Immunohistochemistry (IHC) staining was performed on kidney sections from five mice per group, with the experiment independently repeated three times. Quantification of protein expression was carried out by capturing images from ten random, non-overlapping cortical fields per section using a 40x objective. The staining intensity was semi-quantitatively assessed using the H-Score method: H-Score = Σ (Pi × i), where i represents the intensity score (0: negative; 1: weak; 2: moderate; 3: strong) and Pi is the percentage of cells stained at each intensity.

Relationship Between Glycosylation Hub Genes and Clinical Characteristics

To evaluate the clinical implication of hub genes, data on their association with serum creatinine, eGFR, and proteinuria were provided by the online resource Nephroseq (https://www.nephroseq.org/resource/login.html, V5).

Statistical Analysis

All analyses were performed using R software (version 4.4.2) with pertinent packages and GraphPad Prism 9.0. Student's t-test was applied to analyze the comparisons between groups of continuous variables that were normally distributed, and the Mann–Whitney test was applied for non-normally distributed variables. A two-tailed p-value < 0.05 was considered statistically significant unless otherwise specified. Pearson correlation analysis was applied to assess the relationships between hub gene expression and immune cell infiltration levels. The diagnostic efficacy of each hub gene was evaluated by Receiver Operating Characteristic (ROC) curve analysis, and the area under the curve (AUC) was calculated. AUC values are reported as point estimates along with their 95% confidence intervals (CI), calculated using the DeLong method.

Results

Identification of DEGs and Enrichment Analysis

Two microarray datasets were normalized by preprocessCore R package to remove systematic bias (Figure 1A and B). Then, DEGs were identified with limma package and visualized via the heatmap and volcano plot (Figure 1C-F). A total of 1123 up-regulated DEGs and 873 down-regulated DEGs were screened in GSE30529. A total of 506 up-regulated DEGs and 410 down-regulated DEGs were screened in GSE104954. The Venn diagram was employed to display the intersection of up-regulated or down-regulated DEGs followed by GO terms and KEGG pathway analyses. In the intersecting sets, 339 up-regulated genes and 169 down-regulated genes were obtained (Figure 2A and B). In the GO biological process category, most genes were associated with leukocyte mediated immunity, regulation of peptidase activity, and regulation of endopeptidase activity. For cellular component category, the most enriched terms included collagen-containing extracellular matrix, external side of plasma membrane, and secretory granule lumen. Last, glycosaminoglycan binding, sulfur compound binding, and peptidase regulator activity were the top three largest categories of molecular function (Figure 2C). To elucidate the prominent pathways that these DEGs were involved in, KEGG enrichment analysis was retrieved. As shown in Figure 2D, enriched pathways included phagosome, cell adhesion molecules, tuberculosis, and Epstein-Barr virus infection.

Identification of Glycosylation-Related DEGs

To acquire the differentially expressed glycosylation-related genes in DN, we took the intersecting sets of DEGs and glycosylation genes. As a result, 12 up-regulated glycosylation genes and 3 down-regulated glycosylation genes were represented (Figure 3A and B). To throw light on the functions of glycosylation genes in DN, Gene Ontology (GO) analysis was carried out. As shown in Figure 3C and D, protein glycosylation, macromolecule glycosylation, glycoprotein biosynthetic process and glycoprotein metabolic process were involved in the most highly enriched biological processes. Collagen-containing extracellular matrix was involved in the most highly enriched cellular component. Glycosyltransferase activity, UDP-glycosyltransferase activity and hexosyltransferase activity were involved in the most highly enriched molecular function. Enriched KEGG pathways included Mucin type O-glycan biosynthesis, Glycosphingolipid biosynthesis-globo and isoglobo series, Glycosphingolipid biosynthesis-ganglio series, Various types of N-glycan biosynthesis, and Other types of O-glycan biosynthesis.

The Expression of Glycosylation-Related DEGs in the Kidney from DN Patients

In the GSE30529 database, 26 glycosylation genes are down-regulated and 49 genes are up-regulated (Figure 4A and B). In the GSE104954 database, 9 glycosylation genes are down-regulated, and 22 genes are up-regulated (Figure 4C and D). Differentially expressed glycosylation-related genes in two datasets are presented in Figure 4E and F. Compared to the control group, twelve glycosylation-related genes, including VCAN, GALNT1, LUM, TUBA1A, GCNT3, THBS2, TUSC3, GALNT7, B4GALT5, HEXB, ADAMTS5, and SPON1, were highly expressed in DN, while CGA, ENTPD5, and ST3GAL1 expression was reduced in the GSE30529 database (Supplementary Table S2). Although the first 13 genes expression exhibited a consistent trend, ENTPD5 and ST3GAL1 showed no significant differences in the GSE104954 database (Figure 4E and F). Owing to the two different analytical approaches, it is plausible that the results of limma difference analysis are different from the results of *t*-test between the two groups. The *t*-test assesses differential expression on a gene-by-gene basis, which can be underpowered and unstable with small sample sizes due to its reliance on individually estimated variances. Limma, however, is specifically designed for high-throughput data. It uses an empirical Bayesian framework to "shrink" the variances of individual genes towards a common value, thereby providing more stable and reliable inference, particularly in studies with limited replicates.

Further Screen for Glycosylation-Related Hub Genes

Since the sample sizes of each dataset were relatively small, the two datasets were then merged, and batch effect removal was realized by the limma and sva R packages. PCA plot was generated on the merged dataset using FactoMineR and factoextra packages in R (Figure 5A and B). As a result, we acquired expression profiles for 17 DN patients and

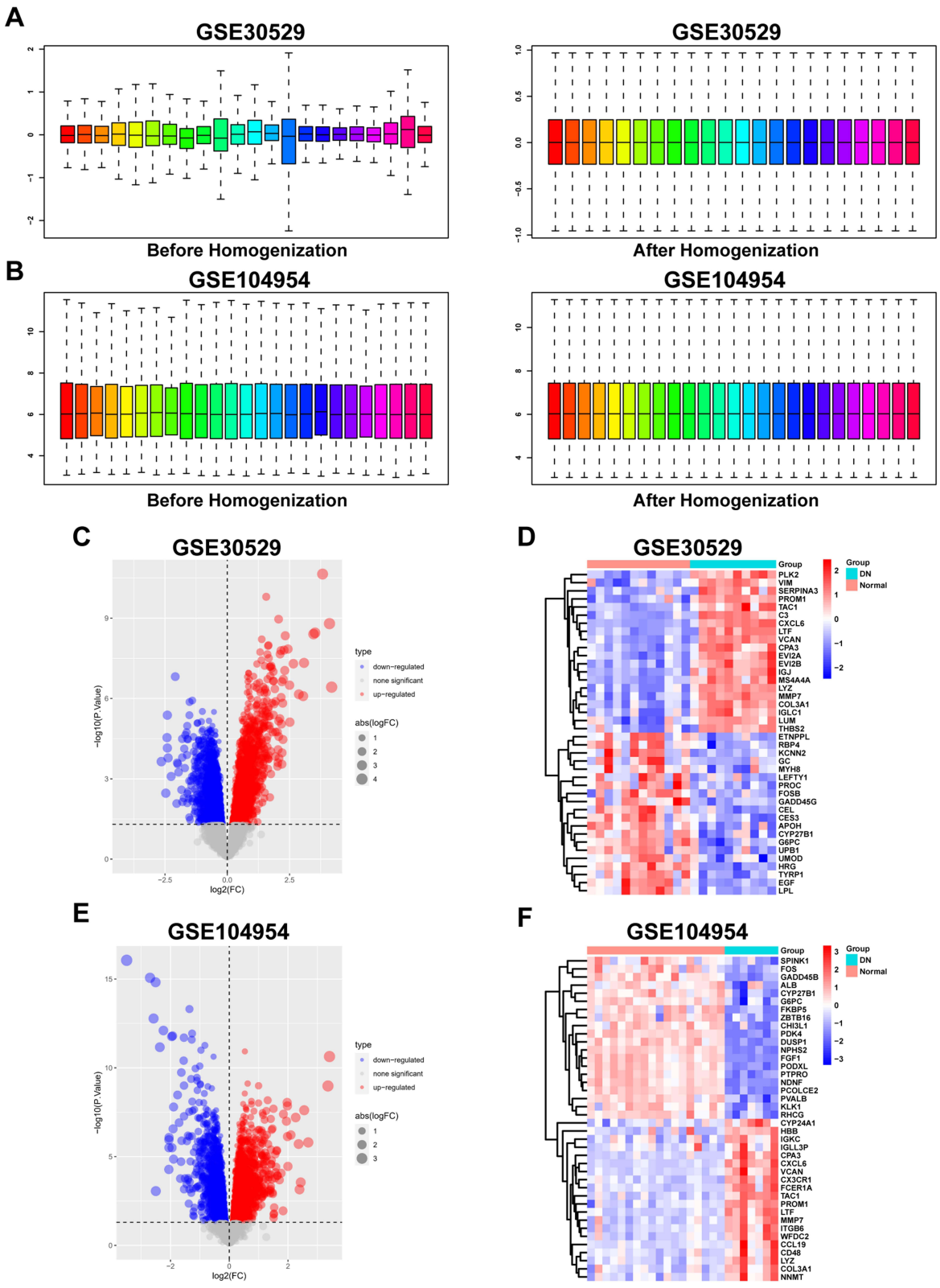

Figure 1 Data processing and identification of DEGs between DN and normal group. (**A** and **B**) Box plots showing the distribution of expression values before and after normalization of datasets GSE30529 and GSE104954. (**C** and **E**) Volcano plots illustrating 1123 significantly up-regulated DEGs and 873 significantly down-regulated DEGs in GSE30529 and 506 significantly up-regulated DEGs and 410 significantly down-regulated DEGs in GSE104954, respectively. (**D** and **F**) Heatmaps displaying the expression patterns of DEGs across DN and normal samples in each dataset.

Abbreviation: DEGs, differentially expressed genes.

https://doi.org/10.2147/IJGM.S545376

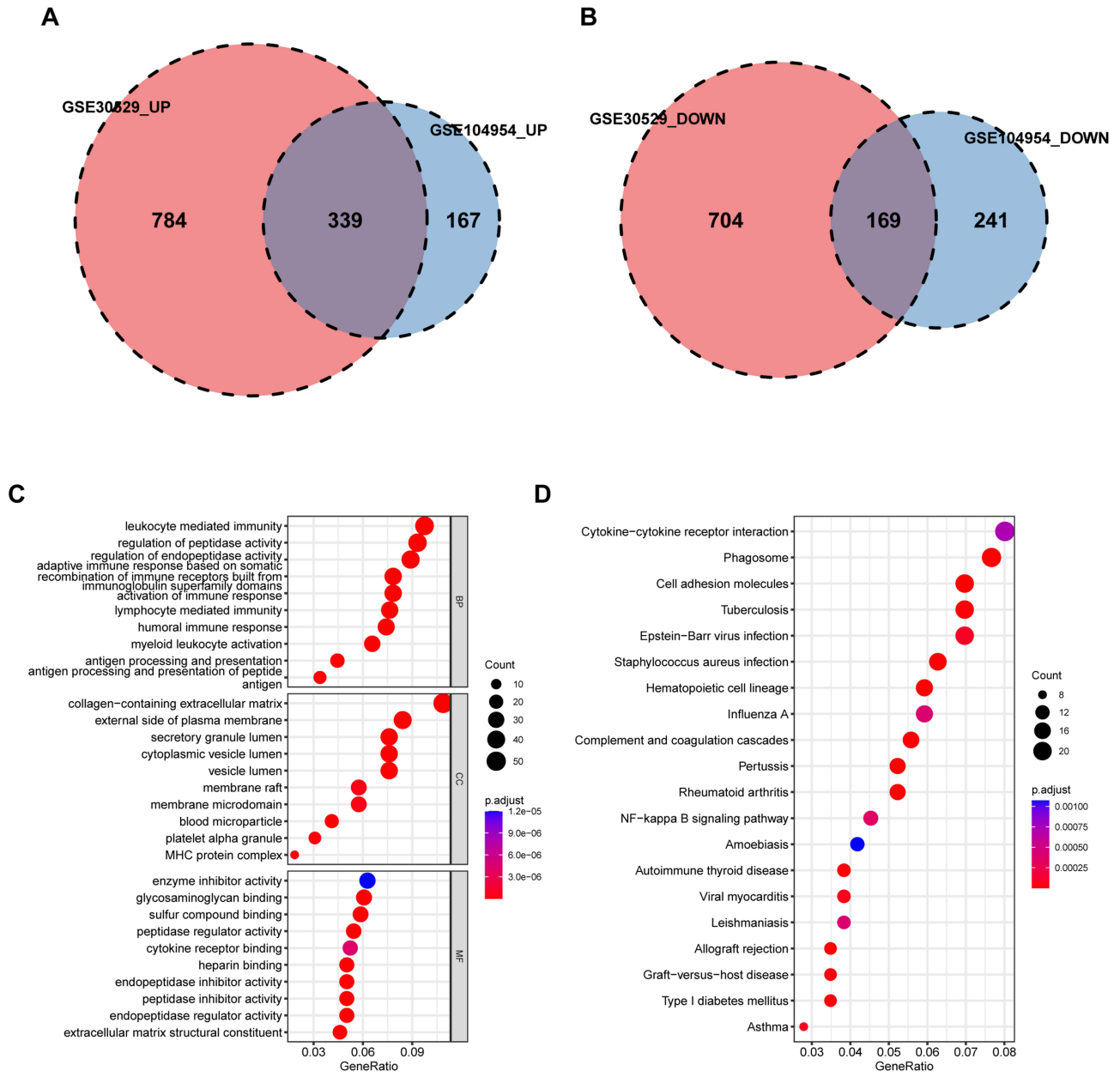

Figure 2 Functional enrichment analysis of common DEGs across two datasets. (**A**) Venn diagram showing 339 common up-regulated DEGs. (**B**) Venn diagram showing 169 common down-regulated DEGs shared between GSE30529 and GSE104954. (**C**) The enriched GO terms of DEGs in molecular function (MF), biological process (BP) and cellular component (CC) categories. (**D**) KEGG pathways enrichment analysis.
Abbreviations: DEGs, differentially expressed genes; GO, gene ontology; KEGG, Kyoto Encyclopedia of Genes and Genomes.

30 healthy controls to perform subsequent analysis. To further narrow down these candidate genes, machine-learning algorithms were tested, including random forest and LASSO regression (Supplementary Table S3 and S4). Combining the DEGs and glycosylation-related gene sets, eight genes (VCAN, GCNT3, TUSC3, GALNT7, B4GALT5, HEXB, ADAMTS5, and CGA) were identified by LASSO method with glmnet R package (Figure 5C). We then screened the top ten genes (B4GALT5, VCAN, GALNT1, GCNT3, GALNT7, CGA, TUBA1A, THBS2, HEXB, and LUM) obtained from random forest analysis using randomForest R package (Figure 5D). An intersection of the genes obtained from the two methods was performed, and six hub genes of glycosylation, namely HEXB, B4GALT5, GALNT7, GCNT3, CGA, and VCAN, were finally selected (Figure 5E). Among these six candidate genes, CGA is down-regulated and other five genes are up-regulated in DN. Among these five up-regulated candidate genes, VCAN is the most highly expressed,

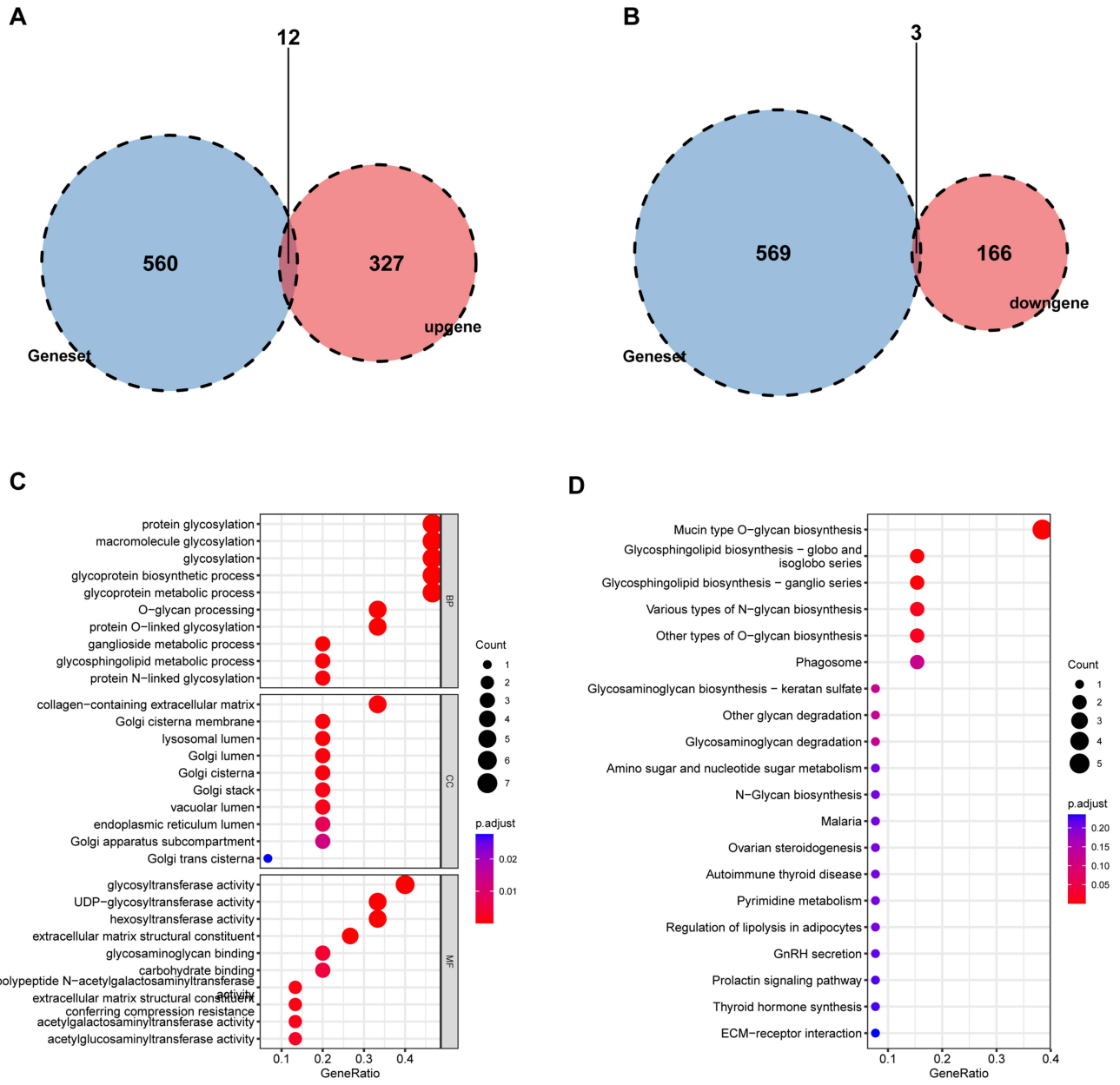

Figure 3 Enrichment analysis of glycosylation-related genes.(**A** and **B**) Venn diagrams showing the overlap between glycosylation-related genes and significantly up-regulated DEGs (**A**) or down-regulated DEGs (**B**). (**C**) GO enrichment analysis of detected glycosylation-related genes in molecular function (MF), biological process (BP) and cellular component (CC). (**D**) KEGG pathway analysis of detected glycosylation-related genes.
Abbreviations: DEGs, differentially expressed genes; GO, gene ontology; KEGG, Kyoto Encyclopedia of Genes and Genomes.

followed by GCNT3 and GALNT7 (Figure 5F). Correlation between hub genes mirrored that the most positively correlated genes were HEXB and GALNT7 (r=0.726038114, p=7.69E-09), and the most negatively correlated genes were VCAN and CGA (r=−0.589895144, p=1.28E-05) (Figure 5G). The performance of the identified six hub genes for the diagnosis of DN was determined through ROC curves. According to the ROC curve, these genes showed a good diagnostic value for DN, with area under the curve (AUC) values as follows: HEXB (AUC = 0.892, 95% CI: 0.800–0.984), B4GALT5 (AUC = 0.909, 95% CI: 0.805–1.000), GALNT7 (AUC = 0.931, 95% CI: 0.842–1.000), GCNT3 (AUC = 0.929, 95% CI: 0.856–1.000), CGA (AUC = 0.898, 95% CI: 0.811–0.985), and VCAN (AUC = 0.967, 95% CI: 0.900–1.000). VCAN was the strongest diagnostic marker for DN with an AUC of 0.967, which was followed by GALNT7 and GCNT3 (Figure 5H and Supplementary Figure S1).

https://doi.org/10.2147/IJGM.S545376

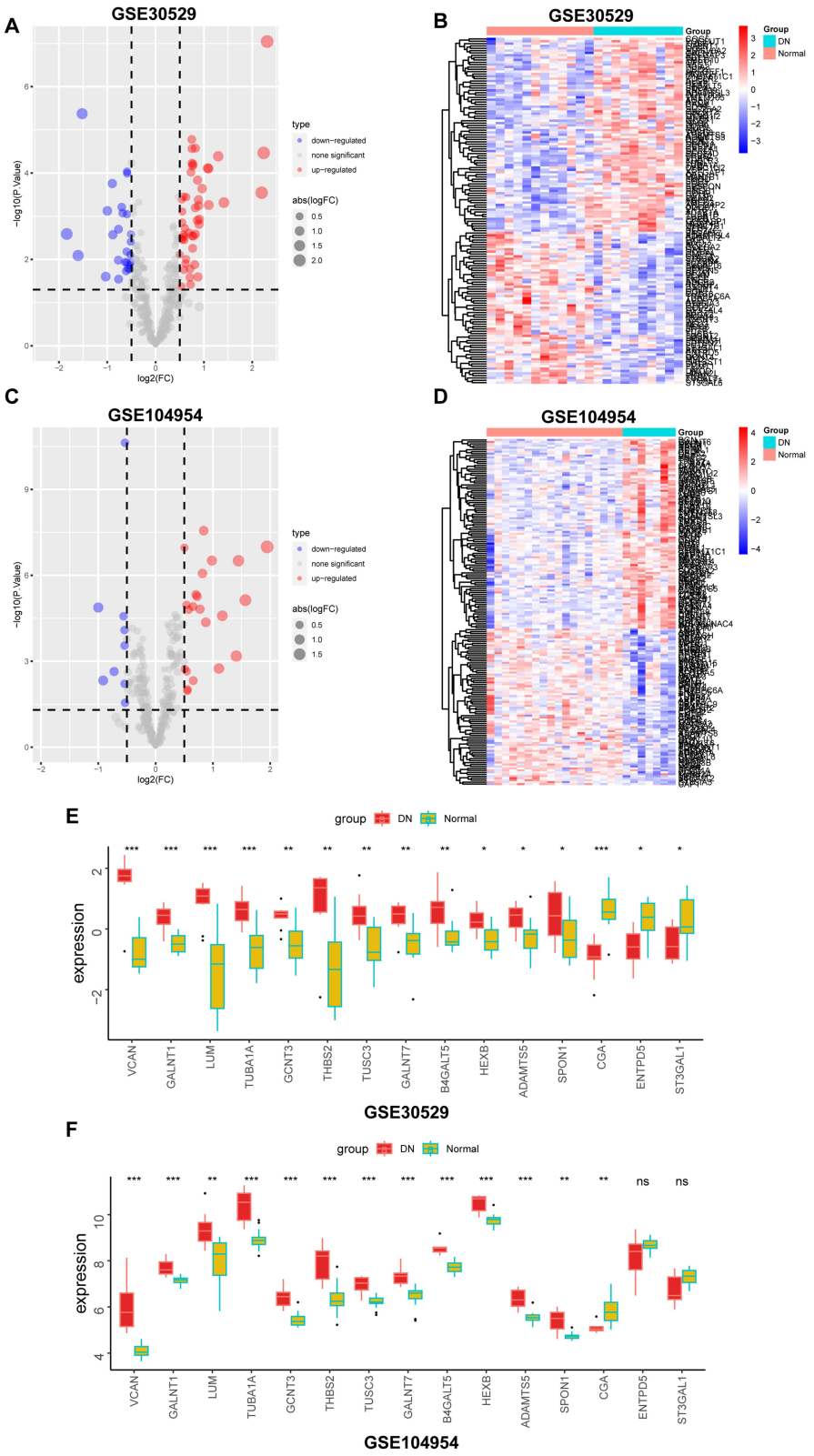

Figure 4 The expression of glycosylation-related genes in DN datasets. (**A** and **C**) Volcano plots highlighting glycosylation-related genes in GSE30529 (**A**) and GSE104954 (**C**). (**B** and **D**) Heatmaps showing expression profiles of glycosylation-related genes. (**E** and **F**) The expression levels of significantly differentially expressed glycosylation-related genes between DN and normal samples in GSE30529 (**E**) and GSE104954 (**F**). *p < 0.05, **p < 0.01, ***p < 0.001. The "ns" indicates not significant.

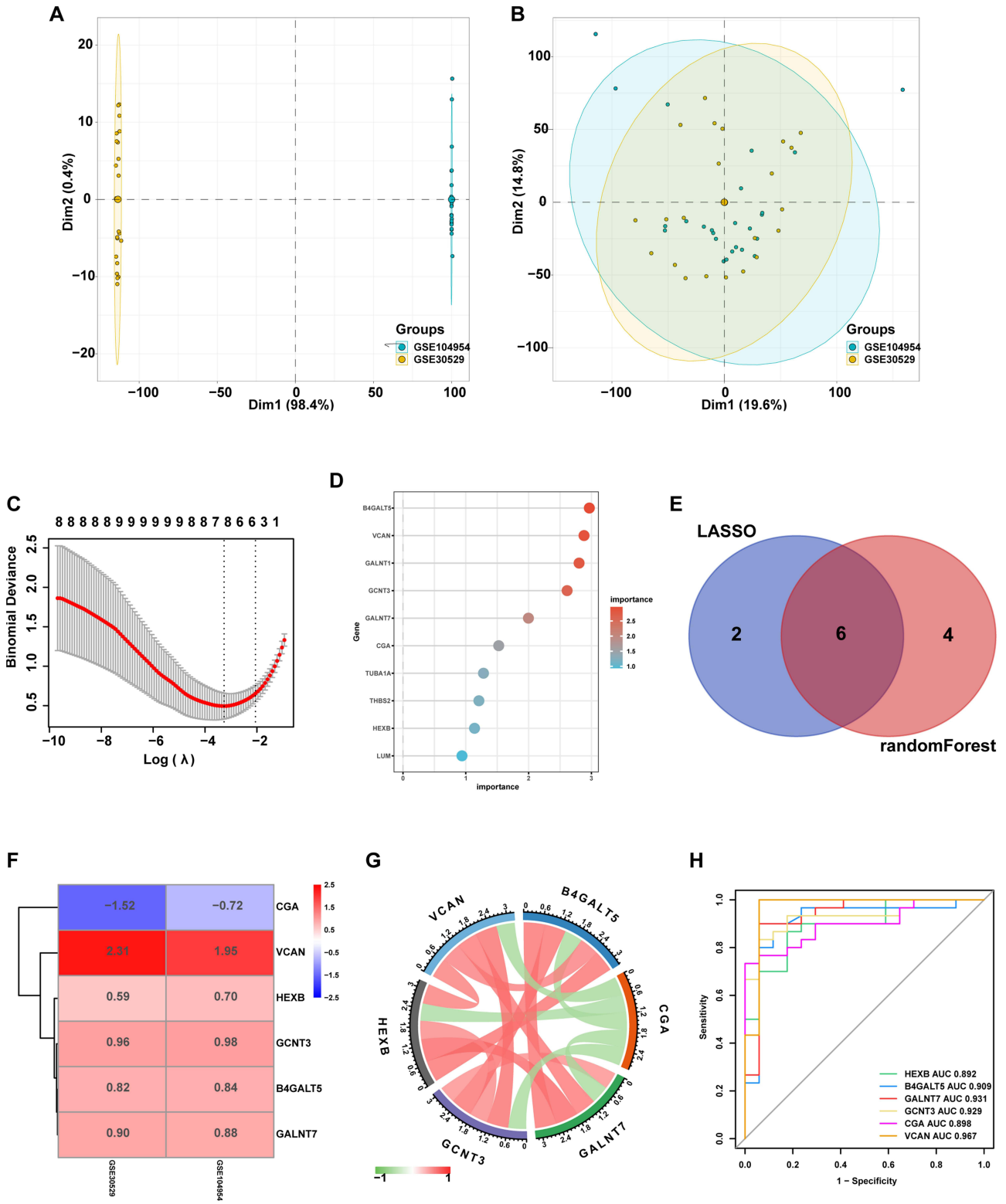

Figure 5 Identification of hub genes using LASSO regression and random forest regression. (**A**) Principal component analysis (PCA) of the unmerged data set. (**B**) Principal component analysis (PCA) of the merged data set. (**C**) The LASSO regression analysis. (**D**) The top ten genes selected from the random forest algorithm. (**E**) Venn diagram of overlapping hub genes identified by LASSO and random forest. (**F**) Heatmap demonstrating differential expression patterns (logFC values) of six hub genes in the two datasets. (**G**) Correlation analysis among the six hub genes. (Red lines represent positive correlation, whereas green lines represent negative correlation; the darker the color, the greater the correlation). (**H**) ROC curves showing diagnostic efficacy of hub genes for DN.

Abbreviations: LASSO, least absolute shrinkage and selection operator; ROC, receiver operating characteristic.

https://doi.org/10.2147/IJGM.S545376

Association Between Hub Genes and Immune Signature

Subsequently, we conducted immune cell infiltration analysis to evaluate the abundance of different immune cell infiltration in DN patients and the normal individuals. We demonstrated the correlations among various immune cell subsets which indicated immature B cells were significantly negatively correlated with Type 17 helper cells. In addition, among the infiltrating cells, it is MDSCs that were most closely related to other immune cells (Figure 6A). The immune cells with a remarkably higher proportion of infiltration in DN included activated CD4 T cell, activated B cell, activated dendritic cell, Gamma delta T cell, immature B cell, Macrophage, Mast cell, MDSC, Natural killer cell, Natural killer T cell, Regulatory T cell, T follicular helper cell, Type 1 T helper cell, and Type 2 T helper cell, while the immune cells with a remarkably lower proportion of infiltration in DN included immature dendritic cell and Neutrophil compared to healthy group (Figure 6B). Analysis of the immune microenvironment revealed distinct patterns with clear clinical implications. Specifically, DN group, characterized by a dominant Macrophage signature, is associated with the deterioration of renal function and the progression of interstitial fibrosis. This signature has been widely reported to predict disease progression in DN.[16,17] Although other immune cells also play important roles in the disease process, the evidence for their direct association with clinical indicators, particularly as independent prognostic predictors, still requires further research. We investigated the correlation between six hub genes and infiltrating immune cells. The results indicated that VCAN was positively correlated with the infiltration of Regulatory T cell, Natural killer cell, and Activated dendritic cell. The three infiltrating cells most closely related to HEXB were Gamma delta T cell, Type 1 T helper cell and activated CD8 T cell. The three infiltrating cells most closely related to GCNT3 were natural killer cell, activated dendritic cell and regulatory T cell. The three infiltrating cells most closely related to GALNT7 were Gamma delta T cell, Type 2 T helper cell and activated CD8 T cell. CGA was positively correlated with the infiltration of neutrophil, and negatively correlated with the infiltration of activated CD8 T cell and natural killer cell. B4GALT5 was positively correlated with Type 1 T helper cell, Type 2 T helper cell and activated CD4 T cell (Figure 7 and Supplementary Table S5).

Construction of Co-Expression Network and Gene Set Enrichment Analysis (GSEA)

After determining six hub genes, we performed a correlation analysis between hub genes and other genes. The heatmaps showed the top 50 genes that were positively associated with each of the six hub genes, respectively (Figure 8). Based on the results of correlation analysis above, Single-gene GSEA using Reactome was conducted, and the top 20 terms were shown in Figure 9. According to the results, the related genes mainly focus on the immune system and inflammatory response. B4GALT5 expression was positively correlated with immune system disorders and negatively correlated with mitochondrial protein import. CGA expression was negatively correlated with Antigen presentation: folding, assembly and peptide loading of class I MHC and S phase. GALNT7 expression was positively associated with integrin cell surface interactions. GCNT3 expression was positively correlated with Syndecan interactions, Non-integrin membrane-ECM interactions, and ECM proteoglycans. HEXB expression showed a positive correlation with host interactions of HIV factors. VCAN expression exhibited positive correlation with generation of second messenger molecules and interferon alpha/beta signaling (Figure 9). This GSEA revealed distinct immune and inflammatory pathways associated with each hub gene (Supplementary Table S6).

Construction of Transcription Factor (TF)-miRNA-mRNA Interactions

Finally, to demonstrate the potential regulators of these hub genes, we predicted upstream transcription factors (TFs) and miRNAs via Regnetwork database and constructed the hub gene-associated miRNA and TFs network. The regulatory network consisted of 42 TFs, 99 miRNAs, 51 gene-TF interaction pairs and 111 gene-miRNA pairs (Figure 10). The gene-TFs regulatory network was constructed to determine core TFs and their effect on the hub genes. As a result, TFAP2A was identified as the pivotal TF to modulate the three hub genes: B4GALT5, HEXB, and CGA. Other TFs, including FOS, FOXA1, JUN, MAX, TP53, USF1, and USF2, were also identified as important regulators of these target genes. No upstream regulatory factors for GCNT3 were identified in the Regnetwork database. In this study, some miRNAs play a key role in modulating these hub genes. Hsa-miR-101 may regulate the expression of CGA and VCAN.

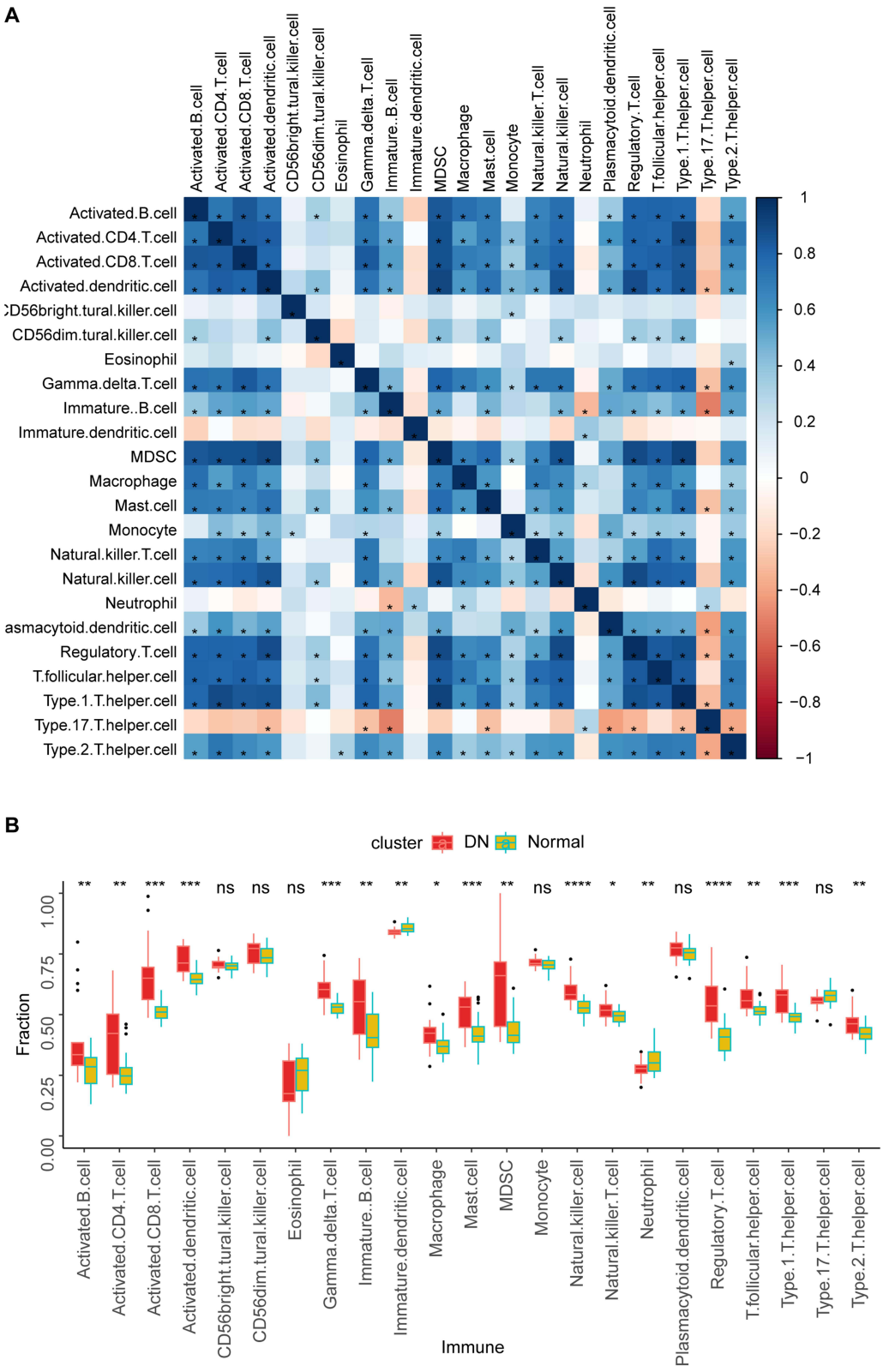

Figure 6 Immune cell infiltration analysis in DN. (**A**) Correlation among infiltrating immune cells. (**B**) The disparity of infiltrated immune cells between the DN group and the normal group. *p < 0.05, **p < 0.01, ***p < 0.001. The "ns" indicates not significant.

https://doi.org/10.2147/IJGM.S545376

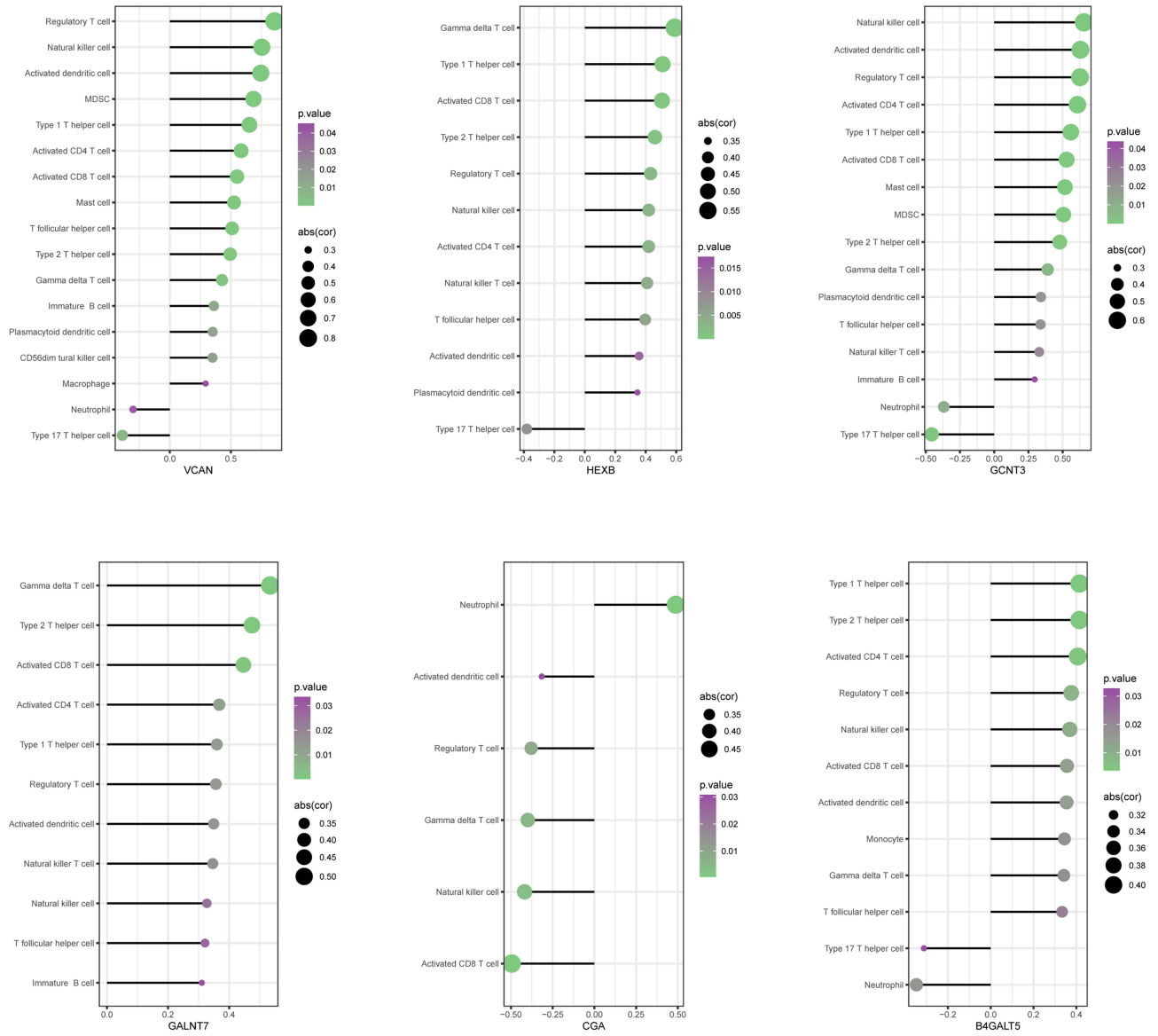

Figure 7 Correlation of hub genes expression with the infiltration levels of diverse immune cell types.

Hsa-miR-30a was predicted to be involved in regulating B4GALT5 and GALNT7. In addition, hsa-miR-508-3p was found to regulate HEXB and CGA. The results demonstrate that different genes can be regulated by the same miRNA.

The Expression Levels and Clinical Significance of Hub Genes

The expression of CGA mRNA was significantly decreased in DN patients, while the mRNA expression of the other five hub genes was significantly increased in the two databases. Furthermore, the protein expression levels of six hub molecules in DN mice kidney tissues yielded similar results (Figure 11). As shown in Figure 11, six hub gene-encoded proteins were predominantly expressed in tubular epithelial cells, and these protein level changes were consistent with the change in mRNA expression. To investigate the potential effect of hub genes on the prognosis of DN, the publicly available database Nephroseq was employed. In the Nephroseq data set, the abundance of VCAN in the tubulointerstitium was positively correlated with serum creatinine (r = 0.671, Figure 12A) and negatively correlated with GFR (r=−0.627, Figure 12B) in DN patients. Moreover, VCAN expression had a positive association with proteinuria (r=0.784, Figure 12C) in DN patients. GCNT3 expression showed a negative correlation with GFR in DN patients (r=

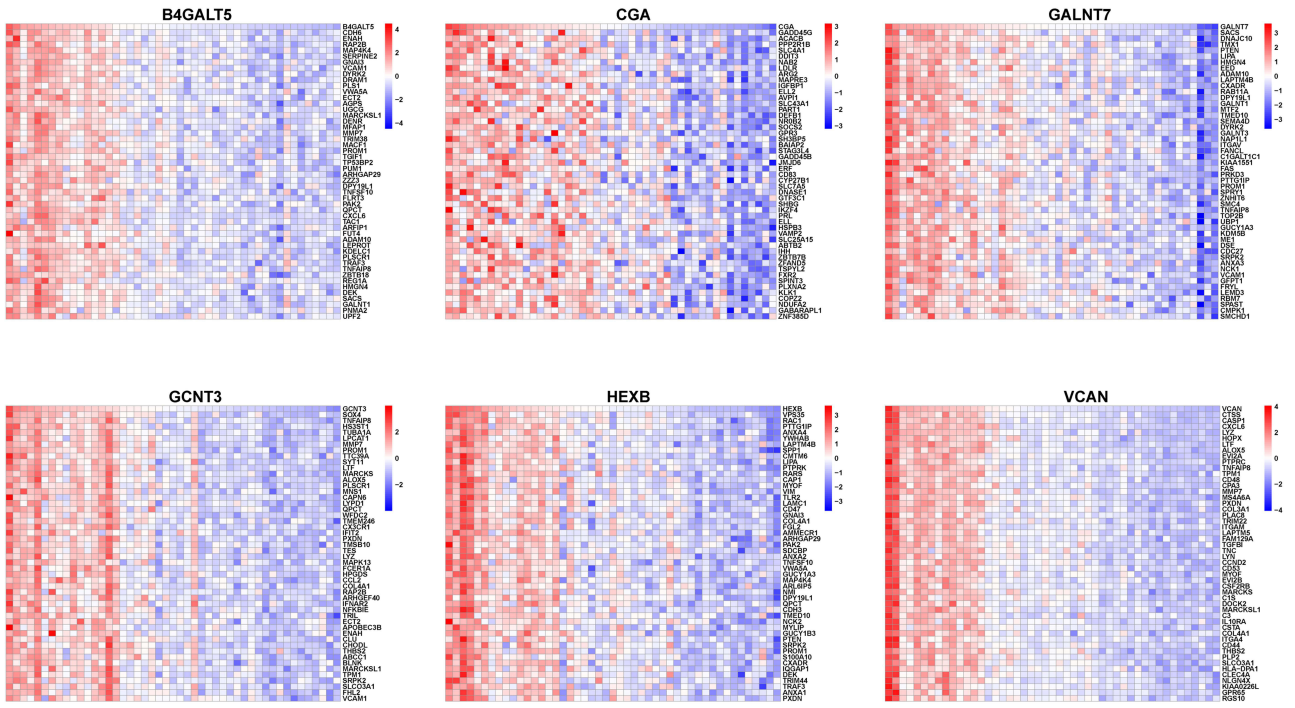

Figure 8 Heatmap displaying the top 50 most positively correlated genes with each hub gene.

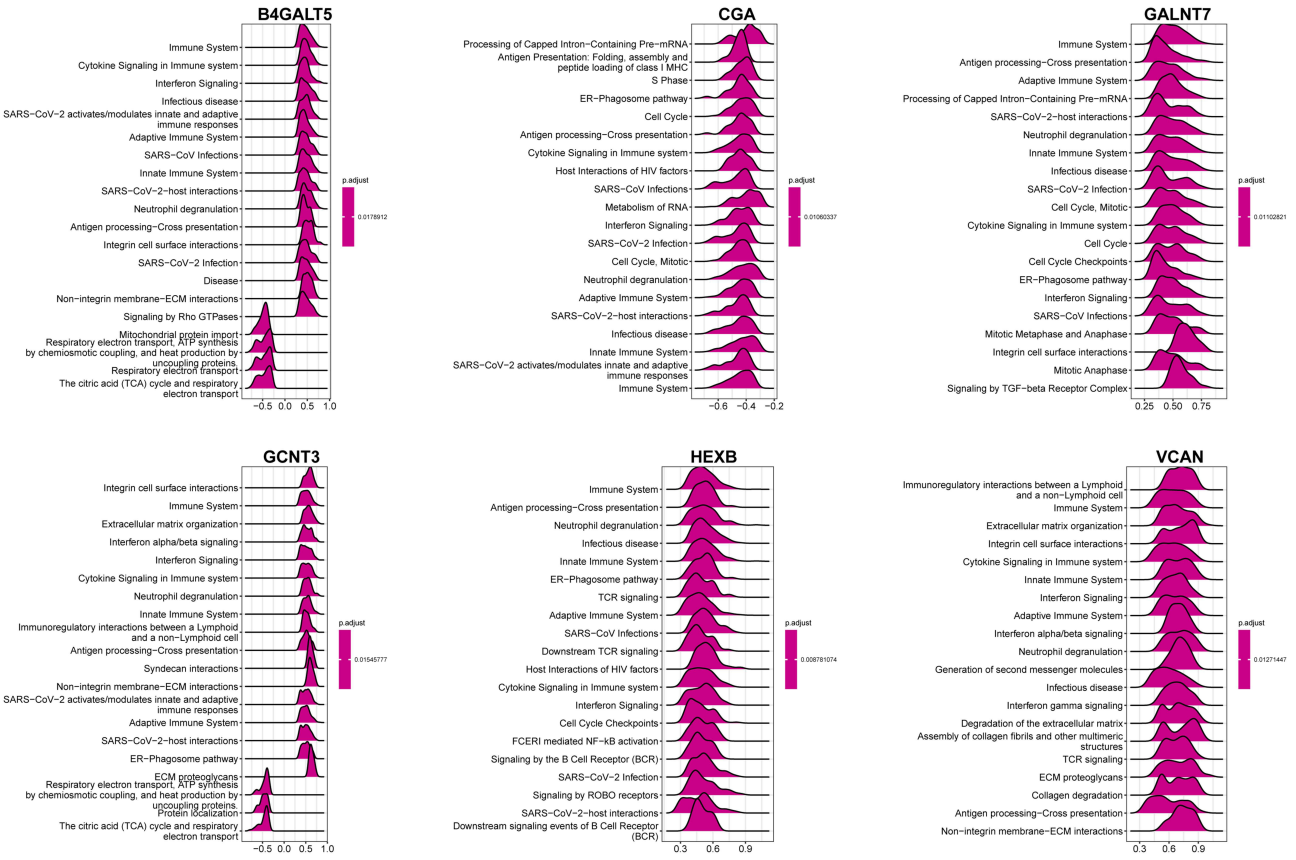

Figure 9 GSEA was performed based on the Reactome Database, and the top 20 pathways were displayed.

https://doi.org/10.2147/IJGM.S545376

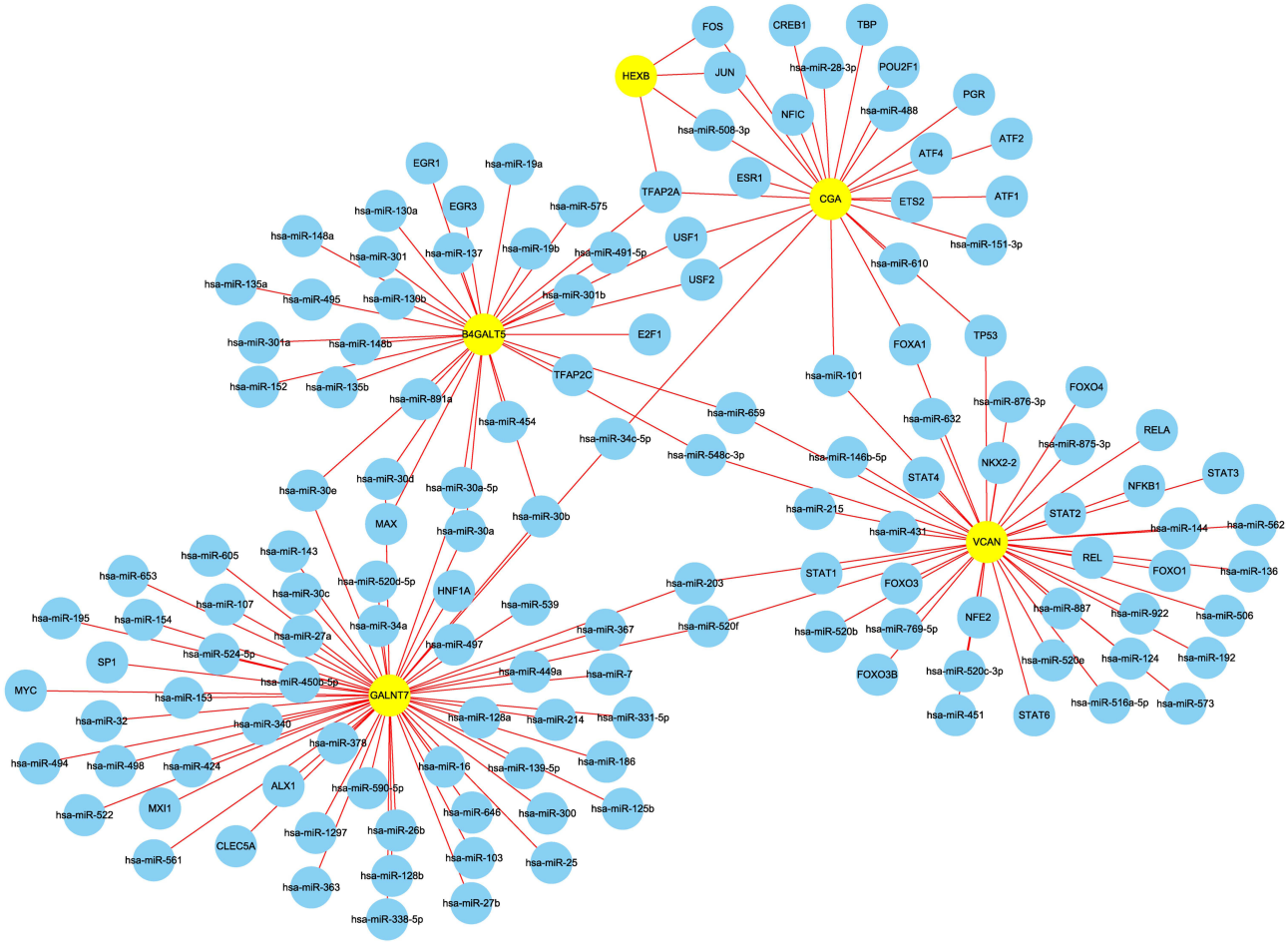

Figure 10 Predicted upstream transcription factors and miRNAs by the RegNetwork Database.

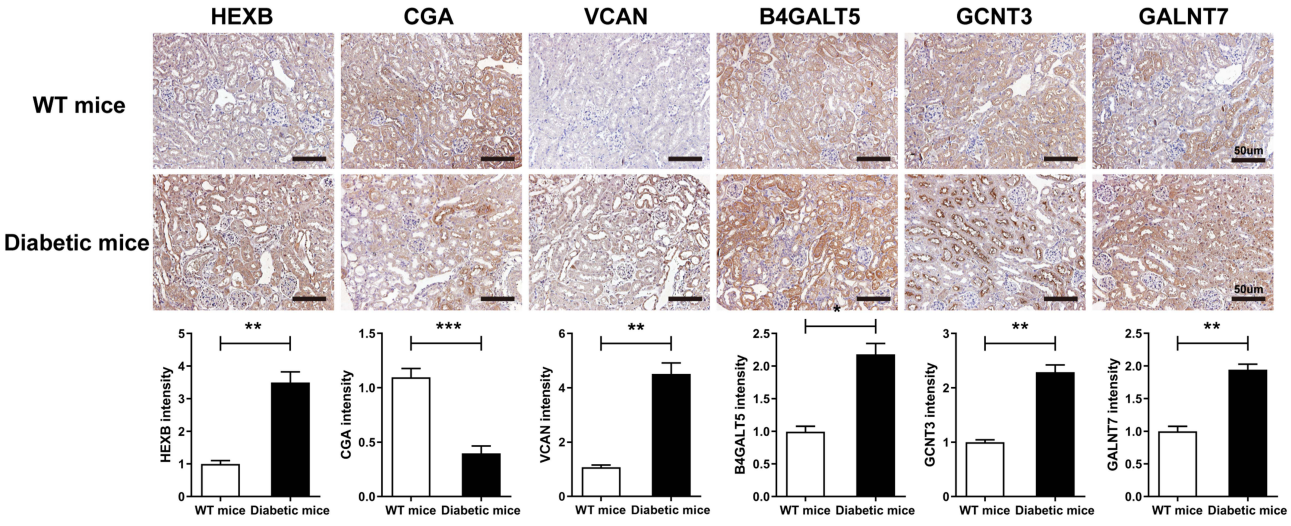

Figure 11 Validation of hub genes by immunohistochemistry. Scale bar, 50um. *p < 0.05, **p < 0.01, ***p < 0.001.

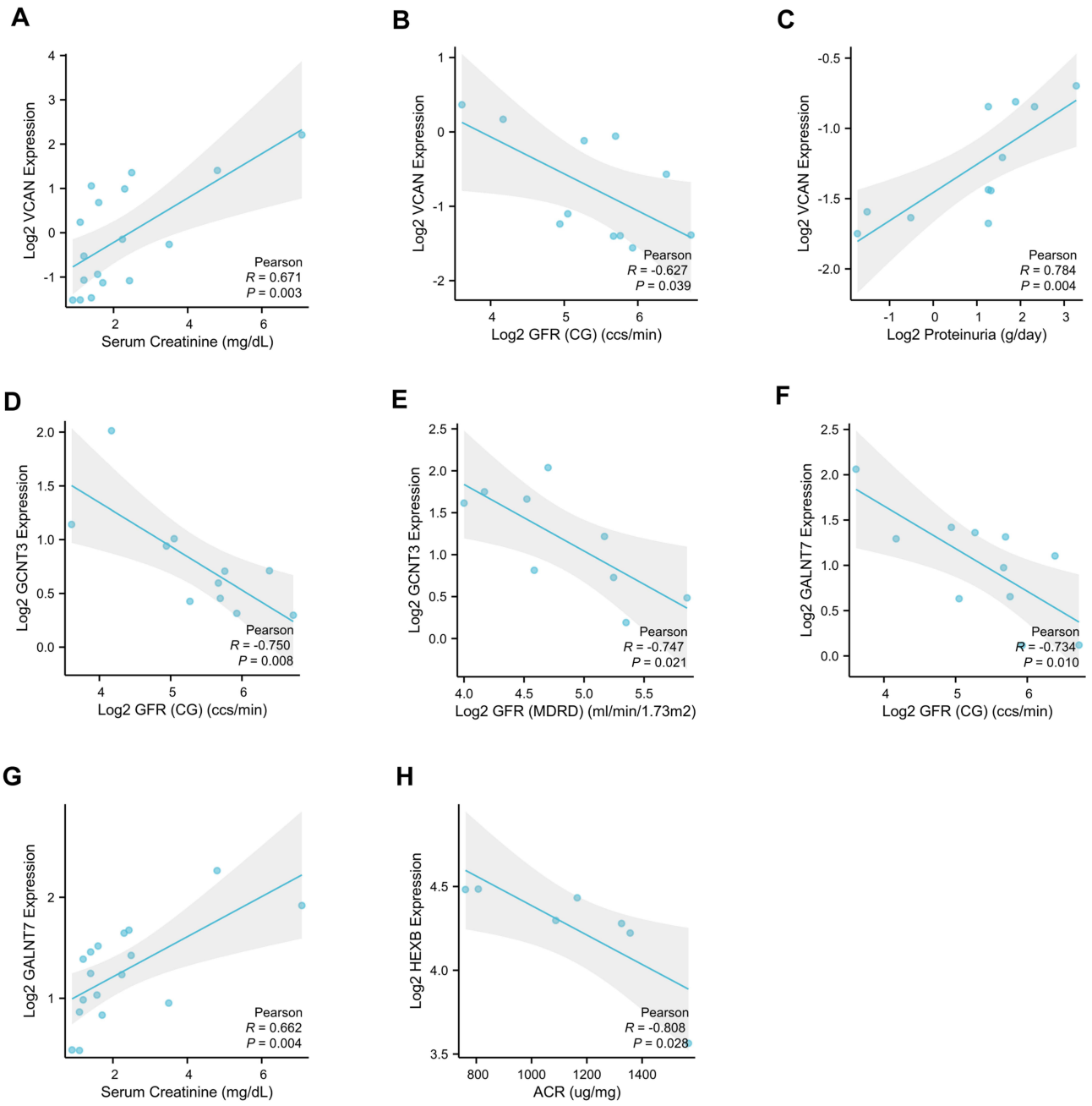

Figure 12 Correlation of hub genes expression and clinical measures. Correlation between VCAN expression and serum creatinine level (**A**), GFR (**B**), and proteinuria (**C**) in DN patients and normal controls. Correlation between GCNT3 expression and GFR-CG (**D**) and GFR-MDRD (**E**) in DN patients and normal controls. Correlation between GALNT7 expression and GFR (**F**) and serum creatinine level (**G**) in DN patients and normal controls. (**H**) Correlation between HEXB expression and ACR in eNOS-deficient C57BLKS db/db mice.

−0.750, Figure 12D) (r=−0.747, Figure 12E). GALNT7 expression was negatively correlated with GFR (r=−0.734, Figure 12F) and positively correlated with serum creatinine (r=0.662, Figure 12G) in DN patients. HEXB expression was negatively correlated with ACR (r=−0.808, Figure 12H) in diabetic nephropathy mouse model. Human clinical metrics concerning HEXB, B4GALT5, and CGA were not available in the database.

Discussion

DN, the primary cause of ESRD, is characterised histopathologically by mesangial matrix expansion, glomerulosclerosis, and tubulointerstitial fibrosis. Multiple factors contribute to the onset and progression of DN, including inflammation

https://doi.org/10.2147/IJGM.S545376

processes, immune system disorders, oxidative stress and post-translational modifications. Post-translational modifications, including acetylation, methylation, ubiquitination, and lactylation, have been proven to be involved in many diseases, such as autoimmune disorders, inflammation, neurodegenerative diseases, and oncological diseases. Nevertheless, there are few studies on the role of glycosylation in tubular injury of DN. Glycosylation is the most common protein modification by which a glycan is covalently attached to the target proteins and produce an effect on its function. Excess or aberrant glycosylation is closely associated with the production of advanced glycation end products (AGEs).[18,19] ROS can promote glycation reactions and this is known as glycoxidation.[20] AGEs not only stimulate the formation of extracellular matrix and subsequent fibrosis, but also induce epithelial-mesenchymal transition (EMT) and ER stress in proximal renal tubular epithelial cells through binding to their receptors.[21] Recent studies further underscores the importance of glycosylation in renal fibrosis.[22,23] Consequently, this study aims to identify glycosylation-associated hub genes, and clarify its role and clinical implications in DN by a comprehensive bioinformatics analysis.

Six glycosylation-related hub genes, namely B4GALT5, CGA, GALNT7, GCNT3, HEXB, and VCAN, were identified via taking the overlap of the results from DEGs, a glycosylation-related gene set, and the machine learning algorithms. B4GALT5 (beta-1,4-galactosyltransferase5) belongs to a member of beta-1,4-glycosyltransferase (B4GALT) gene family, and catalyzes the formation of lactosylceramide by accelerating the transformation of galactose from UDP-galactose to GlcCer.[24] It has been proven that B4GALT5 serves as an important determinant in neurodevelopment, tumor formation, and immune and inflammatory responses.[25] It is reported that downregulation of B4GALT5 mitigates insulin resistance via decreasing the accumulation of M1 macrophages and increasing adipogenesis in HFD-fed mice and ob/ob mice.[26] However, the role of B4GALT5 in renal diseases is unreported, and its function remains uncharacterized. In our study, we found B4GALT5 was closely related to T helper cells and activated CD4+ T cell, indicating its significant role in regulating inflammatory and immunomodulatory responses. Further, GSEA analysis of B4GALT5-coexpressed genes also confirms this. CGA (glycoprotein hormones, alpha polypeptide) encodes the alpha subunit of the glycoprotein hormone family. Elevated expression of CGA is observed in ER-positive breast cancer, pancreatic cancer, gastric cancer and prostate cancer.[27–29] It is found that a CGA/EGFR/GATA2 circuit was involved in chemoresistant gastric cancer.[30] CGA was down-regulated in the tubulo-interstitium of DN and showed high diagnostic value for DN with a high area under the ROC curve. GALNT7 (polypeptide N-acetylgalactosaminyltransferase 7) is a glycosyltrans-ferase and responsible for O-linked glycosylation initiatation by transferring N-acetylgalactosamine. It is reported that the expression of GALNT7 is higher in HER2-positive, PR-positive or ER-positive breast cancer. Moreover, high expression of GALNT7 indicates a good prognosis in a HER2-dependent manner in patients with breast cancer.[31] SPDEF gives rise to the tumorigenesis and a poor outcome by directly facilitating the transcript level of GALNT7 in luminal breast cancer.[32] GALNT7-medicated aberrant glycosylation in many cancers is involved in various biological processes including cell proliferation, differentiation, invasion, metastasis and immune surveillance.[33,34] Our findings revealed that significantly expressed GALNT7 in DN had a high diagnostic value and was negatively associated with declined kidney function, indicating GALNT7 may be a good diagnostic biomarker and a risk factor for the progression of DN. O-glycan is closely associated with cell growth, invasion, migration, and metastasis. GCNT3 (N-Acetylglucosaminyl- transferase 3) is up-regulated O-glycan synthase in castration-resistant prostate cancer, which may became a potential therapeutic target.[35] Decreased GCNT3 expression is closely associated with a high risk of recurrence in colon cancer patients.[36] In this study, GCNT3 was intimately linked to natural killer cell and ECM proteoglycans, indicating that GCNT3 may involve in natural killer cell-mediated pro-inflammatory immune environment as well as ECM-induced kidney fibrosis in DN. β-Hexosaminidases (β-Hex) serve as a series of glycosyl hydrolase isozymes and can remove GalNAc or GlcNAc residues from macromolecules in the lysosomes. Two subunits, α subunit and β subunit, can compose three distinct hexosaminidase isozymes, including HexA, HexB, and HexS. β-hex can break down sialylated and neutral glycosphingolipids in the lysosomes to protect against its accumulation in neuronal cells.[37] It was found that HEXB deficient zebrafish exhibited aberrant lysosomes in microglia, glial progenitors and neuronal cells.[37]

VCAN (Versican) is a highly abundant chondroitin sulphate proteoglycan that plays a critical role in matrix remodelling, progression and malignant transformation in many solid tumours. Although distinct subtypes of VCAN are tissue and disease-specific, they possess the same function, such as accelerating cell adhesion, proliferation, and migration. It is found that VCAN is highly expressed in blood and bone marrow of multiple myeloma patients, indicating a good diagnostic efficiency.[38] miR-144 and miR-199 can decrease the expression of VCAN, thus inhibiting FAK/STAT3

signaling pathway and restraining multiple myeloma.[39] There is evidence that VCAN is implicated in a decrease in the number of intraepithelial CD8+ T cells and increased depth of cervical invasion.[40] In addition, VCAN is involved not only in proliferation and migration of vascular smooth muscle cell, but also in its phenotypic change and elastogenesis inhibition after vessel injury.[41] Feng et al demonstrate that VCAN can boost cardiomyocyte hyperplasia and heart repair by regulating integrin β1, ERK1/2 and Akt signalling pathway.[40] A recent study reveals that VCAN can drive the expression of Nos2 and aortic disease in an Akt pathway-dependent manner.[42] Of the identified six hub genes, VCAN was most closely related to immune cell infiltration, indicating the key role of VCAN in immunomodulatory mechanism. The expression of VCAN was positively correlated with the infiltration of regulatory T cells, natural killer cells, activated dendritic cells. It is found that versican-derived matrikines facilitate the differentiation of dendritic cells and enhance the infiltration of T cells in colorectal cancer.[43] Notably, the role of VCAN in immune infiltration of DN has not yet been determined. Immune dysfunction, inflammatory state, enhanced mesangial matrix and fibrosis are the primary mechanisms which trigger the initiation and progression of DN. GSEA method based on VCAN-coexpressed genes using Reactome database demonstrated that these genes were mainly enriched in immune system, metabolism, and innate immune system. Consistently, VCAN may play a vital role in promoting DN, and the exact molecular mechanisms need further exploration. Our results reveal that there is a strong correlation between VCAN and interferon alpha/beta signaling, suggesting that VCAN may possess a pro-inflammatory effect and the potential molecular mechanism remains to be explored. Moreover, VCAN exhibited the best diagnostic efficiency in distinguish DN from healthy individuals, demonstrating that VCAN may be a promising biomarker of DN.

It has been detected that an increased number of immune cells in kidneys from early diabetic nephropathy patients consist of monocytes, plasma cells, B cells, and T cells.[44] Single-cell transcriptomic analyses conducted in the kidney from mouse model with early type 1 diabetic nephropathy threw light on macrophage subtypes transformation and gene expression alteration in different phenotype.[45] The pivotal role of immune cells and inflammation in the pathogenesis and progression of DN has been well established by a lot of evidence.[46,47]

Evidence supports that glycosylation-related genes is associated with the function of infiltrating immune cells. Inhibition of FUT8-mediated core fucosylation blocked Smad2/3 and ERK signaling pathway, thereby exerting a renoprotective effect in DN.[48] Targeting sialylation, a cancer-associated glycosylation, can repolarize tumor-associated macrophages and produce effective checkpoint blockade, restraining tumor progression.[49] It was found that prosaposin hyperglycosylation in tumor dendritic cells resulted in cancer immune escape.[50] Inhibition of O-glycosylation in tumor cells triggered the M1 type conversion in macrophages and potentiated T-cell-mediated cytotoxicity in head and neck cancer, illustrating that O-glycosylation governs cancer-immune-cell crosstalk.[51] In innate immunity-related diseases, neutrophil glycosylation modulates its effector functions including chemotaxis, phagocytosis, and degranulation.[52] Increasing lines of evidence showed that glycosylation also modulates the development of T and B cells.[53] Few studies, however, have investigated the relationship between glycosylation-related genes and immune cells in DN. In this study, all of six hub genes are closely associated with immune cells infiltration into kidney with diabetic nephropathy, suggesting they may involve in the immunological and inflammatory response underlying the development of diabetic nephropathy. Further, the exact molecular mechanisms of these effects remain to be characterized with further investigation.

Currently, the diagnosis of DN relies heavily on invasive renal biopsy, which is viewed as the gold standard. Therefore, it is essential for early diagnosis of DN to develop noninvasive, accurate, and specific biomarkers. In this study, six hub genes have the potential to be considered as markers for distinguishing DN patients from normal subjects effectively. Further studies are entailed to elucidate the specific function and potential mechanisms of these glycosylation-related hub genes. To corroborate these findings, we validated the expression of these six hub genes in vivo experimental models, which were consistent with those of our bioinformatics analysis results. We then investigated the predictive value of these selected hub genes in clinical conditions. According to the nephroseq database, the elevated expression of VCAN, GCNT3 and GALNT7 were positively correlated with renal function decline of DN patients, demonstrating that they may exert adverse effects in the progression of DN and lead to a poor prognosis. To date, other three hub genes have not been explored in subjects with diabetic nephropathy. Therefore, further research exploring their clinical significance and specific mechanisms of action is warranted.

The high diagnostic AUC values, particularly for VCAN, GALNT7, and GCNT3, suggest their potential as non-invasive biomarkers to complement or even reduce reliance on invasive renal biopsies for early DN detection. This functional insight distinguishes our candidates from classical inflammatory cytokines like TNF-α or IL-6, which are broad indicators of inflammation. Our hub genes, however, point to more specific immunological mechanisms that may underlie the chronic inflammatory state in DN. Furthermore, the positive correlation of VCAN, GCNT3, and GALNT7 with declining renal function in patient cohorts positions them as potential prognostic indicators. Therapeutically, these hub genes represent novel targets. For example, targeting the enzymatic activity of GALNT7 or GCNT3 with small-molecule inhibitors could disrupt the glycosylation-dependent signaling that promotes fibrosis and immune dysfunction. Monoclonal antibodies against VCAN or its derived matrikines could be explored to modulate the immune microenvironment in DN.

Our study, however, has some limitations. First, the in vivo validation, while consistent, was confined to a single mouse model (STZ-induced) and a modest sample size. Future studies should include validation in other models (eg, db/db) and in human serum or urine samples to assess their true clinical utility as liquid biopsy biomarkers. Second, further functional experiments are warranted to elucidate the precise molecular mechanisms by which these glycosylation-related genes influence immune cell behavior and renal fibrosis in DN.

Conclusions

This study is among the first to elucidate the significant role of glycosylation-related genes in the onset and progression of DN, identifying six hub genes with substantial diagnostic potential. Importantly, our findings underscore the crucial role of glycosylation in the immune-related mechanisms of DN, offering novel insights into the disease's pathogenesis and opening avenues for immunomodulatory therapeutic strategies. The incorporation of these glycosylation-based biomarkers into existing diagnostic frameworks may markedly enhance the accuracy of non-invasive diagnosis and improve risk stratification in clinical practice. Furthermore, this work highlights the promise of glycosylation-related genes as prognostic biomarkers and potential targets for intervention. Moving forward, future research should focus on validating these genes in larger cohorts, delineating their precise molecular mechanisms in DN pathophysiology, and exploring their utility in personalized treatment approaches to ultimately improve patient outcomes.

Abbreviations

DN, Diabetic nephropathy; ESRD, End-stage renal disease; GEO, Gene Expression Omnibus; DEGs, Differentially expressed genes; GO, Gene Ontology; KEGG, Kyoto Encyclopedia of Genes and Genomes; LASSO, Least absolute shrinkage and selection operator; PCA, Principal component analysis; ROC, Receiver Operating Characteristic; AUC, The area under the curve; ssGSEA, single-sample Gene set enrichment analysis.

Data Sharing Statement

The datasets analyzed in the current study are available from the public online Gene Expression Omnibus (GEO) database. GSE30529: https://www.ncbi.nlm.nih.gov/geo/query/acc.cgi?acc=GSE30529. GSE104954: https://www.ncbi.nlm.nih.gov/geo/query/acc.cgi?acc=GSE104954.

Ethics Statement

According to the national legislation of China, specifically Items 1 and 2 of Article 32 of the Measures for Ethical Review of Life Science and Medical Research Involving Human Subjects (issued on February 18, 2023), this research utilizing publicly available, de-identified data is exempt from ethical approval. The animal study was reviewed and approved by the Ethical Committee of the First Affiliated Hospital of Zhengzhou University. All animal experiments were carried out following the National Standard of Animal Care and Use Procedures.

Acknowledgments

We acknowledge the financial support from the Postdoctoral Research Foundation of the First Affiliated Hospital of Zhengzhou University.

Author Contributions

All authors made a significant contribution to the work reported, whether that is in the conception, study design, execution, acquisition of data, analysis and interpretation, or in all these areas; took part in drafting, revising or critically reviewing the article; gave final approval of the version to be published; have agreed on the journal to which the article has been submitted; and agree to be accountable for all aspects of the work.

Funding

This study was supported by the National Natural Science Foundation of China (No. 82400845) and the Fundamental Research Funds for the Central Universities of Central South University (2024ZZTS0513).

Disclosure

The authors declare that they have no competing interests.

References

1. Rimesh P, Sanjay KB. AGEs accumulation with vascular complications, glycemic control and metabolic syndrome: a narrative review. *Bone*.. 2023;176.PMID: 37598920
2. Jeongmin L, Jae-Seung Y, Seung-Hyun K. Advanced glycation end products and their effect on vascular complications in type 2 diabetes mellitus. *Nutrients*. 2022;14(15).PMID: 35956261
3. Colin R, Tyler JS, Matthew BR, Jan N. Glycosylation in health and disease. *Nat Rev Nephrol*. 2019;15(6).PMID: 30858582
4. Katrine TS, Yoshiki N, Hiren JJ, Henrik C. Global view of human protein glycosylation pathways and functions. *Nat Rev Mol Cell Biol*. 2020;21 (12).PMID: 33087899
5. Dušan V, Christopher RA. Spatial glycomics and kidney disease. *Semin Nephrol*. 2025;44(6).PMID: 40210529
6. Weifu R, Qi B, Yan C. Mass spectrometry-based N-glycosylation analysis in kidney disease. *Front Mol Biosci*. 2022;9.PMID: 36072428
7. Juraj K, Hertzel CG, Paul JB, Peter DR. Advanced glycation end products predict loss of renal function and high-risk chronic kidney disease in type 2 diabetes. *Diabetes Care*. 2022;45(3).PMID: 35051276
8. Puneet G, Ton R. Glomerular proteinuria: a complex interplay between unique players. *Adv Chronic Kidney Dis*. 2011;18(4).PMID: 21782129
9. Di L, Xi C, Hao W, et al. The changes of immunoglobulin G N-glycosylation in blood lipids and dyslipidaemia. *J Transl Med*. 2018;16(1). PMID: 30157878.
10. L RFH, Marija V, Daniel U, et al. IgG glycan patterns are associated with type 2 diabetes in independent European populations. *Biochim Biophys Acta Gen Subj*. 2017;1861(9). PMID: 28668296.
11. Zhiyuan W, Haibin L, Di L, et al. IgG glycosylation profile and the glycan score are associated with type 2 diabetes in independent chinese populations: a case-control study. *J Diabetes Res*. 2020;2020. PMID: 32587867.
12. S SS, Ralph H, Claudia KEM, et al. Association of the IgG N-glycome with the course of kidney function in type 2 diabetes. *BMJ Open Diabetes Res Care*. 2020;8(1). PMID: 32349995.
13. Dinko Š, Jerko Š, Marko T, et al. Human complement component C3 N-glycome changes in type 1 diabetes complications. *Front Endocrinol*. 2023;14. PMID: 37293493.
14. Mengyun X, Zigan X, Xiaohui Z, et al. Immunological profiling in type 2 diabetes mellitus and type 2 diabetic kidney disease: insights from single-cell LacNAc sequencing. *Front Endocrinol*. 2025;16. PMID: 40862112.
15. Gabriela B, Bernhard M, Marie T, et al. Spatiotemporal dynamics of intratumoral immune cells reveal the immune landscape in human cancer. *Immunity*. 2013;39(4). PMID: 24138885.
16. Ozcan U, Cihan H, Fatma Sema Anar K, et al. Relationship between complement and macrophage markers with kidney survival in patients with diabetic nephropathy. *Acta Diabetol*. 2025. PMID: 40338344.
17. K CQF, Malu Z, Ron W, et al. Macrophages in diabetic nephropathy in patients with type 2 diabetes. *Nephrol Dial Transplant*. 2016;32 (8):325–332. [PMID: 27416772]. doi:10.1093/ndt/gfw001
18. Maxime F, Frédéric B, Alexis D. Glycation damage: a possible hub for major pathophysiological disorders and aging. *Aging Dis*. 2018;9(5).PMID: 30271665
19. Anna P, Antonio G, Jubina B, Federico M. Advanced Glycation End Products (AGEs): biochemistry, signaling, analytical methods, and epigenetic effects. *Oxid Med Cell Longev*. 2020;2020. PMID: 32256950
20. Izabela S-B, Grzegorz B. Effect of glycation inhibitors on aging and age-related diseases. *Mech Ageing Dev*. 2016;160. PMID: 27671971
21. Kuo-How H, Siao-Syun G, Wei-Han L, et al. Role of calbindin-d28k in diabetes-associated advanced glycation end-products-induced renal proximal tubule cell injury. *Cells*. 2019;8(7). PMID: 31262060.
22. Bingxue Q, Yang C, Siyang C, Xiaodan L, Li K. O-linked β-N-acetylglucosamine (O-GlcNAc) modification: emerging pathogenesis and a therapeutic target of diabetic nephropathy. *Diabet Med*. 2024;42(2).PMID: 39279604
23. Lifen X, Yuxia Z, Guifang W, et al. The UDPase ENTPD5 regulates ER stress-associated renal injury by mediating protein N-glycosylation. *Cell Death Dis*. 2023;14(2). PMID: 36849424.
24. Maryam R, vE RJ, Tanit LG, et al. Adipocytes harbor a glucosylceramide biosynthesis pathway involved in iNKT cell activation. *Biochim Biophys Acta Mol Cell Biol Lipids*. 2019;1864(8). PMID: 31051284.
25. Lei Z, Jie R, Peidian S, et al. The immunological regulation roles of porcine β-1, 4 Galactosyltransferase V (B4GALT5) in PRRSV Infection. *Front Cell Infect Microbiol*. 2018;8. PMID: 29546034.
26. Shu-Fen L, Cui-Song Z, Yu-Meng W, et al. Downregulation of β1,4-galactosyltransferase 5 improves insulin resistance by promoting adipocyte commitment and reducing inflammation. *Cell Death Dis*. 2018;9(2). PMID: 29415997.

27. B I, P B, LD V, et al. Identification of CGA as a novel estrogen receptor-responsive gene in breast cancer: an outstanding candidate marker to predict the response to endocrine therapy. *Cancer Res*. 2001;61(4). PMID: 11245479.
28. Hua H, Ruining P, Yue Z, et al. L3MBTL2-mediated CGA transcriptional suppression promotes pancreatic cancer progression through modulating autophagy. *iScience*. 2022;25(5). PMID: 35521536.
29. Ivan B, Alain L, Béatrice P, et al. CGA gene (coding for the alpha subunit of glycoprotein hormones) overexpression in ER alpha-positive prostate tumors. *Eur Urol*. 2002;41(3). PMID: 12180238.
30. Cao T, Lu Y, Wang Q, et al. A CGA/EGFR/GATA2 positive feedback circuit confers chemoresistance in gastric cancer. *The Journal of Clinical Investigation*. 2022;132(6). PMID: 35289315. doi:10.1172/JCI154074
31. Berkel C, Cacan E. The expression of O-linked glycosyltransferase GALNT7 in breast cancer is dependent on estrogen-, progesterone-, and HER2-receptor status, with prognostic implications. *Glycoconjugate Journal*. 2023;40(6):631–644. [PMID: 37947928]. doi:10.1007/s10719-023-10137-4
32. Li J, Wan X, Xie D, et al. SPDEF enhances cancer stem cell-like properties and tumorigenesis through directly promoting GALNT7 transcription in luminal breast cancer. *Cell Death & Disease*. 2023;14(8):569. [PMID: 37633945]. doi:10.1038/s41419-023-06098-z
33. Scott E, Hodgson K, Calle B, et al. Upregulation of GALNT7 in prostate cancer modifies O-glycosylation and promotes tumour growth. *Oncogene*. 2023;42(12):926–937. [PMID: 36725887]. doi:10.1038/s41388-023-02604-x
34. Hua S, Li H, Liu Y, Zhang J, Cheng Y, Dai C. High expression of GALNT7 promotes invasion and proliferation of glioma cells. *Oncology Letters*. 2018;16(5):6307–6314. [PMID: 30405766]. doi:10.3892/ol.2018.9498
35. Daiki Y, Katsumasa S, Takeo K, Mototsugu O, Toshinori S. Functional analysis of GCNT3 for cell migration and EMT of castration-resistant prostate cancer cells. *Glycobiology*. 2022;32(10).PMID: 35867813
36. Margarita G-V, Teodoro V, Juan M-R, et al. Clinical relevance of the differential expression of the glycosyltransferase gene GCNT3 in colon cancer. *Eur J Cancer*. 2014;51(1). PMID: 25466507.
37. Katherine SB, Maia MC, Don JM, Michael T, Michael NGJ. Crystal structure of β-hexosaminidase B in complex with pyrimethamine, a potential pharmacological chaperone. *J Med Chem*. 2011;54(5).PMID: 21265544
38. Nidhi G, Rehan K, Raman K, Lalit K, Alpana S. Versican and its associated molecules: potential diagnostic markers for multiple myeloma. *Clin Chim Acta*. 2015;442.PMID: 25623955
39. Nidhi G, Raman K, Tulika S, Bhavuk G, Alpana S. Targeting of stromal versican by miR-144/199 inhibits multiple myeloma by downregulating FAK/STAT3 signalling. *RNA Biol*. 2019;17(1).PMID: 31532704
40. Arko G, Henry JZ, Hestia VG, Baptist T, Gert JF, Ekaterina SJ. Versican expression is associated with tumor-infiltrating CD8-positive T cells and infiltration depth in cervical cancer. *Mod Pathol*. 2010;23(12).PMID: 20729814
41. Robert H, Mervyn JM, Kathleen B, et al. Inhibition of versican synthesis by antisense alters smooth muscle cell phenotype and induces elastic fiber formation in vitro and in neointima after vessel injury. *Circ Res*. 2005;98(3). PMID: 16385080.
42. María Jesús -R-R, Jorge O, Sara -M-M, et al. Versican accumulation drives Nos2 induction and aortic disease in Marfan syndrome via Akt activation. *EMBO Mol Med*. 2024;16(1). PMID: 38177536.
43. Chelsea H, E PB, Athanasios P, et al. Versican-derived matrikines regulate batf3-dendritic cell differentiation and promote t cell infiltration in colorectal cancer. *J Immunol*. 2017;199(5). PMID: 28754680.
44. Parker CW, Haojia W, Yuhei K, et al. The single-cell transcriptomic landscape of early human diabetic nephropathy. *Proc Natl Acad Sci U S A*. 2019;116(39). PMID: 31506348.
45. Jia F, Zeguo S, Xuan W, et al. The single-cell landscape of kidney immune cells reveals transcriptional heterogeneity in early diabetic kidney disease. *Kidney Int*. 2022;102(6). PMID: 36108806.
46. Sydney CWT, Wai Han Y. Innate immunity in diabetic kidney disease. *Nat Rev Nephrol*. 2020;16(4).PMID: 31942046
47. Greg HT. Diabetic nephropathy - is this an immune disorder? *Clin Sci*. 2017;131(16).PMID: 28760771
48. Ming F, Le K, Xiaolang W, et al. Inhibition of core fucosylation limits progression of diabetic kidney disease. *Biochem Biophys Res Commun*. 2019;520(3). PMID: 31623829.
49. S MA, Natalia RM, Nicole K, et al. Targeting cancer glycosylation repolarizes tumor-associated macrophages allowing effective immune checkpoint blockade. *Sci Transl Med*. 2022;14(669). PMID: 36322632.
50. Pankaj S, Xiaolong Z, Kevin L, et al. Hyperglycosylation of prosaposin in tumor dendritic cells drives immune escape. *Science*. 2024;383(6679). PMID: 38207022.
51. Mei-Chun L, Ya-Ting C, Hsin-Yi W, et al. Targeting tumor O-glycosylation modulates cancer-immune-cell crosstalk and enhances anti-PD-1 immunotherapy in head and neck cancer. *Mol Oncol*. 2023;18(2). PMID: 37452653.
52. Julian U, Sayantani C, Morten T-A. Structural and functional diversity of neutrophil glycosylation in innate immunity and related disorders. *Mol Aspects Med*. 2020;79. PMID: 32847678
53. Manuel MV, Eduarda L-G, P SS. Glycome dynamics in T and B cell development: basic immunological mechanisms and clinical applications. *Trends Immunol*. 2023;44(8).PMID: 37407365